

B. TECH. PROJECT REPORT

On

Synthesis of Multi Colour Emissive Tunable Carbon Dots: Anti-Counterfeit and Optoelectronic Applications

BY

SAKSHAM



**DEPARTMENT OF METALLURGY ENGINEERING AND MATERIALS
SCIENCE ENGINEERING
INDIAN INSTITUTE OF TECHNOLOGY INDORE
May 2022**

Synthesis of Multi Colour Emissive Tunable Carbon Dots: Anti- Counterfeit and Optoelectronic Applications

A PROJECT REPORT

*Submitted in partial fulfillment of the
Requirements for the award of the degrees
of*
BACHELOR OF TECHNOLOGY
in

METALLURGICAL ENGINEERING AND MATERIALS SCIENCE

Submitted by:
SAKSHAM

Guided by:
Dr. Mrigendra Dubey
Associate Professor
Department of Metallurgy Engineering and Materials Science

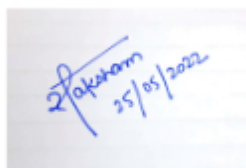


INDIAN INSTITUTE OF TECHNOLOGY INDORE
May 2022

CANDIDATE'S DECLARATION

We hereby declare that the project entitled “**Synthesis of Multi Colour Emissive Tunable Carbon dots: Anti-Counterfeit and Optoelectronic Applications**” submitted in partial fulfilment for the award of the degree of Bachelor of Technology in Metallurgical Engineering and Materials Science completed under the supervision of **Dr. Mrigendra Dubey, Associate Professor, Department of Metallurgy Engineering and Materials Science, IIT Indore** is an authentic work.

Further, I/we declare that I/we have not submitted this work for the award of any other degree elsewhere.



Signature and name of the student(s) with date

CERTIFICATE by BTP Guide(s)

It is certified that the above statement made by the students is correct to the best of my/our knowledge.



Dr. Mrigendra Dubey, Associate Professor IIT Indore

Signature of BTP Guide(s) with dates and their designation

Preface

This report on “Synthesis of Multi Colour Emissive Tunable Carbon Dots: Anti-Counterfeit and Optoelectronic Device Applications” is prepared under the guidance of Dr. Mrigendra Dubey.

Through this report we have tried to synthesis fluorescent carbon dots, and successfully able to tune the fluorescence property of the carbon dots. The synthesized carbon dots show white, purple, cyan, and blue colour fluorescence. We have characterized the carbon dots through FTIR, PL, UV-Vis, ¹H-NMR, ¹³C-NMR, MS, TCSPC, and SEM experiments, and have tried to understand, and explore the mechanism of multicolour emissive carbon dots through these characterizations. Further, these carbon dots are used for anti-counterfeit, and optoelectronic device applications. We are the first to develop UV Converting torch with the help of carbon dot.

We have tried to the best of our abilities and knowledge to explain the content in a lucid manner. We have also models and figures to make it more illustrative.

Saksham

B.Tech. IV Year

Discipline of Metallurgy Engineering and Materials Science

IIT Indore

Acknowledgements

I would like to express my deepest gratitude, and heartiest thankful to my supervisor, Dr. Mrigendra Dubey, for his constant support, intellectual guidance, and motivation during this work. His friendly guidance and expert advice have been invaluable throughout all stages of the work.

I am thankful to my lab mates, Dr. Manish Kumar Dixit, Ms. Moupia Mukherjee, and Mr. Yeeshu Kumar for their continuous support and help throughout the project. The extended discussions and valuable suggestions with the lab members have contributed greatly to the improvement of the thesis.

The people with the greatest indirect contributions to this work are my parents, who have been with me constantly encouraging me throughout this work and in life as well. I would also like to thank the dogs of IIT Indore for cherishing me.

I would also like to thank MEMS Department, SIC IIT Indore for extending instrumental facilities for this work.

Saksham

B.Tech. IV Year

Department of Metallurgy Engineering and Material Science

IIT Indore

Abstract

The tunable photoluminescence (PL) carbon dots (CDs) are synthesized using one-pot solvothermal techniques by varying the $-\text{NH}_2$, $-\text{COOH}$, and $-\text{CH}_2-$ ration on the precursor. The carbon dots were synthesized by using 1, 2, 3, 4- butanetetracarboxylic acid (BTC) along with two groups of reagents: (group 1) aromatic compound by varying the NH_2 : COOH ratio, (group 2): By varying the $-\text{CH}_2-$ on the non-aromatic compound. These carbon dots show white (ABA-CD, ED-CD), purple (AIA-CD), blue (PPD-CD, HYD-CD), and cyan (DBA-CD) colour fluorescence under a single wavelength UV light. The as-obtained carbon dots are further characterized by using ^1H -NMR, ^{13}C -NMR, MS, FTIR, UV-Vis, and PL. The synthesized carbon dots show an optimal fluorescence quantum yield of 37.41% for purple colour emitting carbon dot AIA-CD. The red-shift photoluminescence emission behaviour of purple (AIA-CD), blue (PPD-CD), and cyan colour (DBA-CD) emitting carbon dots can be attributed to the reduction in the bandgap energy from 4.14 to 3.52 to 3.46 eV respectively. Further, the ESI-MS, and ^{13}C -NMR shows that carbon dots can possibly have polymeric structure, and are formed by condensation, and dehydration reactions, along with that carbon dots formed with group 2 precursors have more percentage of sp^3 carbon domains as compared to the carbon dots from group 1. The synthesized carbon dots are further used to manufacture a UV Converting torch which is first of its own kind including white light. Further, due to stability, invisibility under daylight, and low cost these carbon dots are further used for anti-counterfeiting, and information storage applications.

Table of Contents

CANDIDATES' DECLARATION	3
PREFACE	4
Acknowledgement	5
Abstract	6
Chapter 1: Introduction	12-13
1.1 Overview	12
1.2 Carbon Dots	12
1.3 White LEDs	13
Chapter 2: Literature Review	14
2.1 History and Challenges in Carbon Dots	14
2.2 Quantum Confinement Effect	14
Chapter 3: Materials and Methodology	15
3.1 Chemicals and Materials	15
3.2 Equipment and Characterizations	15
Chapter 4: Synthesis	16-17
4.1 Synthesis of Carbon Dots	16
Chapter 5: Results and Discussions	18-27
5.1 Structural Characterization of CD.	18-22
5.1.1 FTIR Analyses	18
5.1.2 ^1H and ^{13}C NMR Analyses	18
5.1.3 Mass Spectroscopic Analyses	20-21

5.2 Morphological Characterization	22
5.3 Optical Characterization	22-27
5.3.1 UV-Vis Absorption Analyses	23
5.3.2 Photoluminescence Study	24
5.3.3 Quantum Yield Measurement	24-25
5.3.4 Time Resolved Photoluminescence Study	25-26
5.3.5 Band Gap Measurements	26-27
Chapter 6: Applications	28-30
6.1 Anti-Counterfeit Application	28-29
6.2 Optoelectronic Application	29-30
Chapter 7: Conclusion and Scope for Future Work	31
7.1 Conclusion	31
7.2 Scope for Future Work	31
References	32-34

List of Figures

- Figure 1:** Schematic of the reaction to form group (1) PPD-CD, DBA-CD, ABA-CD, and AIA-CD, group (2) HYD-CD, and ED-CD. 17
- Figure 2:** FT-IR Analyses of CDs; (a) PPD-CD, (b)DBA-CD, (c) ABA-CD, (d) AIA-CD, (e) HYD-CD, (f) ED-CD. 19
- Figure 3.** (a) $^1\text{H-NMR}$, (b) $^{13}\text{C-NMR}$ of PPD-CD (black line), DBA-CD (red line), ABA-CD (blue line), AIA-CD (green line), HYD-CD (purple line), ED-CD (brown line). 20
- Figure 4:** ESI-MS spectra of CDs (a) PPD-CD, (b)DBA-CD, (c) ABA-CD, (d) AIA-CD, (e) HYD-CD, (f) ED-CD. 21
- Figure 5.** FE-SEM Images of (a). PPD-CD, (b). DBA-CD, (c). ABA-CD, (d). AIA-CD, (e). HYD-CD, (f). ED-CD. 22
- Figure 6.** UV-Vis Spectroscopy Curve of (a) PPD-CD, (b)DBA-CD, (c) ABA-CD, (d) AIA-CD, (e) HYD-CD, (f) ED-CD. 23
- Figure 7.** Photoluminescence Spectra of CDs(a). PPD-CD, (b). DBA-CD, (c). ABA-CD, (d). AIA-CD, (e). HYD-CD, (f). ED-CD. 24
- Figure 8.** TRPL of PPD-CD (black line), DBA-CD (red line), ABA-CD (blue line), AIA-CD (green line), HYD-CD (purple line), ED-CD 1 (brown line), ED-CD 1 (beige line). 26
- Figure 9.** (a) Bandgap energy calculations for PPD-CD (black line), DBA-CD (red line), and AIA-CD (blue line), (b) illustrative scheme to represent the reduction in bandgap resulting in colour modulation. 27
- Figure 10.** (I) Stamp under Visible light (a). PPD-CD, (b). DBA-CD, (c). ABA-CD, (d). AIA-CD, (e). HYD-CD, (f). ED-CD, (II) Stamp under UV Light (a). PPD-CD, (b). DBA-CD, (c). ABA-CD, (d). AIA-CD, (e). HYD-CD, (f). ED-CD. 28-29

Figure 11. Portable light emitting torch (a) Blue Light (PPD-CD), (b) Cyan Light

30

(DBA-CD), (c) White Light (ABA-CD), (d) Purple Light (AIA-CD) (e) Blue Light (HYD-CD),

(f) White Light (ED-CD).

List of Tables

Table 1. Mass Spectra Peaks	20
Table 2. Table 2. Summary of PL decay curves for CDs	26

Chapter 1

Introduction

1.1 Overview

In the real-time, the indispensable need of new energy sources with environment friendly, and non-polluting nature is extremely crucial [1]. Lighting is an integral part of human life and average consumption of light usually falls in the range of 5-20% of total energy for the developed countries [2, 3]. Hence, the continuous evolution in the energy-saving novel light emitting materials is inevitable. In recent times, various light-emitting devices such as light emitting diodes are utilized instead of incandescent and fluorescent lamps owing to their better luminous efficiency, less energy consumption, and longer durability [4]. The most commonly used luminophores for LEDs are Ga-based chips, and rare earth metal-containing yttrium aluminium garnets (YAG) [5, 6]. Despite the high light conversion potential of the mentioned luminophores, lack of abundance as well as expensiveness limits their use [7]. Thus, alternative luminescent materials with desirable properties are demanding candidates for blooming LED industries. Carbon dots (CDs), a new class of fluorescent materials with cost-effectiveness, better light converting efficiency, tunable fluorescence, eco-friendly nature etc., makes them advantageous substitute for the rare earth-mediated luminophores [8, 9].

1.2 Carbon Dots

Carbon dots are 0D nanomaterials. Carbon Dots were first discovered by Xu et. al [10], during the purification of single-walled carbon nanotubes (SWCNTs) through electrophoresis. Carbon Dots are synthesized by various routes which are categorized into two groups: (1). Top-Down approach, where the bigger carbon structures are broken down in order to bring to nanoscale, (2). Bottom-Up approach, which refers to the synthesis of CDs from smaller molecules [11]. Carbon dots because of their nano size usually less than 10 nm, involve the quantum confinement effects, and make them a fluorescent material [12]. Surface properties of carbon dots are varied by doping them with the heteroatom which alters the energy state present in the carbon, and helps in the tuning of fluorescence of carbon dots. [13]. The carbon dots can be synthesized from various raw materials varying from carbon containing items in the nature to chemicals available in the laboratory. [14,15]. Carbon dots are used in various applications including information storage [16], cell imaging [17], fingerprint sensing [18] etc.

1.3 White LEDs

In general, two routes have been followed to produce white LEDs (WLED) either the combination of red, green, and blue colour emitting luminophores [19,20] or the CDs are doped with inorganic compounds (such as ZnO) [21]. Both the strategies come with exploitation of more resources and time, high preparation cost and hazardous to the environment, respectively. In addition to this, fluorescence quenching of CDs during the solid state LED applications is another demanding issue to be studied. Till to date, the CDs have been homogeneously dispersed in silica based polymers, epoxy, PVP, PVA to exclude the possibility of aggregation caused quenching in CDs during solidification due to excess resonance energy transfer or direct π - π interactions.[22-26].

Chapter 2

Literature Review

2.1 History and Challenges in Carbon Dots.

Carbon Dots can be manufactured by using various precursors. For example, Tyagi et. al, synthesized carbon dots by using lemon peel waste as a precursor to get blue colour emission [27]. Carbon dots can be prepared by single precursor or by group of precursors. Ye et. al,[28], used *p*-phenylenediamine as a sole precursor to form red light emitting carbon dots, while Yulong et. al[29], produced carbon dots by using *o*-phenylenediamine, and thiourea as reactants. Carbon dot fluorescence properties can be tuned by various methods which are grouped together to two groups- (1) separation of various colour emitting CDs from a single carbon dot using various chromatographic techniques [30], or (2) by using the different combination of reactants to produce carbon dots [31]. Majorly, most of the fluorescent CDs generate blue, green and yellow emission but obtaining CDs with tunable fluorescence for multicolour emitting LEDs including white light emission is still a major challenge due to Kasha's rule [32]. For example, Susu et. al [33] , synthesized the blue, green, red , and yellow colour emitting carbon dots, mixed the blue, yellow, and red colour carbon dots to get the white LED. For making such White LEDs, experimentalist has to do a lot of experiments to find the optimum ratio of blue, green, and red colour CDs which are giving maximum luminescence in the white colour, which can be achieved only by hit and trial, thus make this path as a very time consuming, and vegetative.

2.2. Quantum Confinement Effect

In a micro/macro size entities, there are many closely packed energy states, which makes them to have continuous energy levels. However in nanomaterials especially carbon dots, the size of dots are almost comparable to the wavelength of the electron. Due to which, these materials possess discrete energy levels, due to which the electrons get confined by the walls of the material, and causing the quantum confinement effect which is making the carbon dots fluorescent.

Chapter 3

Materials and Methodology

3.1 Chemicals and materials

1, 2, 3, 4-Butanetetracarboxylic acid, *p*-Phenylenediamine, 3,5-diaminobenzoic acid, 4-aminobenzoic acid, 4-aminoisophthalic acid, Ethanol, Quinine Sulphate were purchased from Sigma Aldrich Chem. Ltd, Mumbai, India. Ethylene Diamine, Hydrazine Hydrate were bought (TCI chemicals). All the above mentioned chemicals were used as received. 0.22 μm syringe filter papers were required for impurity purification of as-formulated C-dots, purchased from Sigma Aldrich Chem. Ltd, Mumbai, India. UV-LED chip was supplied by Waylone Technologies.

3.2. Equipment and Characterizations

Spectrum Two Perkin Elmer was used for getting FTIR spectra. The electronic absorption and photoluminescence spectra was acquired from UV-vis 2600 Shimadzu and Fluorescence FL8500 Perkin Elmer spectrophotometers respectively. $^1\text{H-NMR}$ spectra were performed on a Bruker AVANCE III 400 Ascend Bruker Bio Spin International AG spectrometer. Electro spray ionization mass (ESI-MS) spectra were recorded on a Waters (Micro mass MS Technologies) Q-tof Premier. FE-SEM analyses was done using a JOEL7610F Plus. For time-resolved decays, a picosecond time-correlated single photon counting (TCSPC) machine from Horiba (Fluorocube-01- NL) was used.

Chapter 4

Synthesis

4.1. Synthesis of Carbon Dots

Briefly, 0.2g of BTC and 0.37g of *p*-phenylenediamine in a molar ratio of 1:4 were put into 10ml of ethanol and transferred to a Teflon-lined stainless autoclave (25ml) which was kept at 200°C for 12hrs in an electric oven for the Solvothermal reaction. After the completion of the reaction, it was brought to room temperature naturally, and then centrifuged at 11000rpm for 30min at room temperature. The collected supernatant was filtered through a 0.22 μ m filter membrane, and the filtrate (PPD-CD) was collected for further analyses. Similarly, 3, 5-diaminobenzoic acid(0.52g), 5-aminoisophthalic acid(0.62g), 4-aminobenzoic acid(0.47g), hydrazine(170 μ l), and ethylenediamine(203 μ l) each along with 0.2g of butanetetracarboxylic acid(0.2g) in the same molar ratio of 4:1 put into 10ml of ethanol, and above experiment was repeated under same reaction conditions to get DBA-CD, AIA-CD, ABA-CD, HYD-CD, and ED-CD, respectively. Due to aromatic structure of the reactant, PPD-CD, DBA-CD, AIA-CD, ABA-CD are grouped to group 1 carbon dots, and HYD-CD and ED-CD are grouped to group 2. Fig 1 shows the schematic of the reaction.

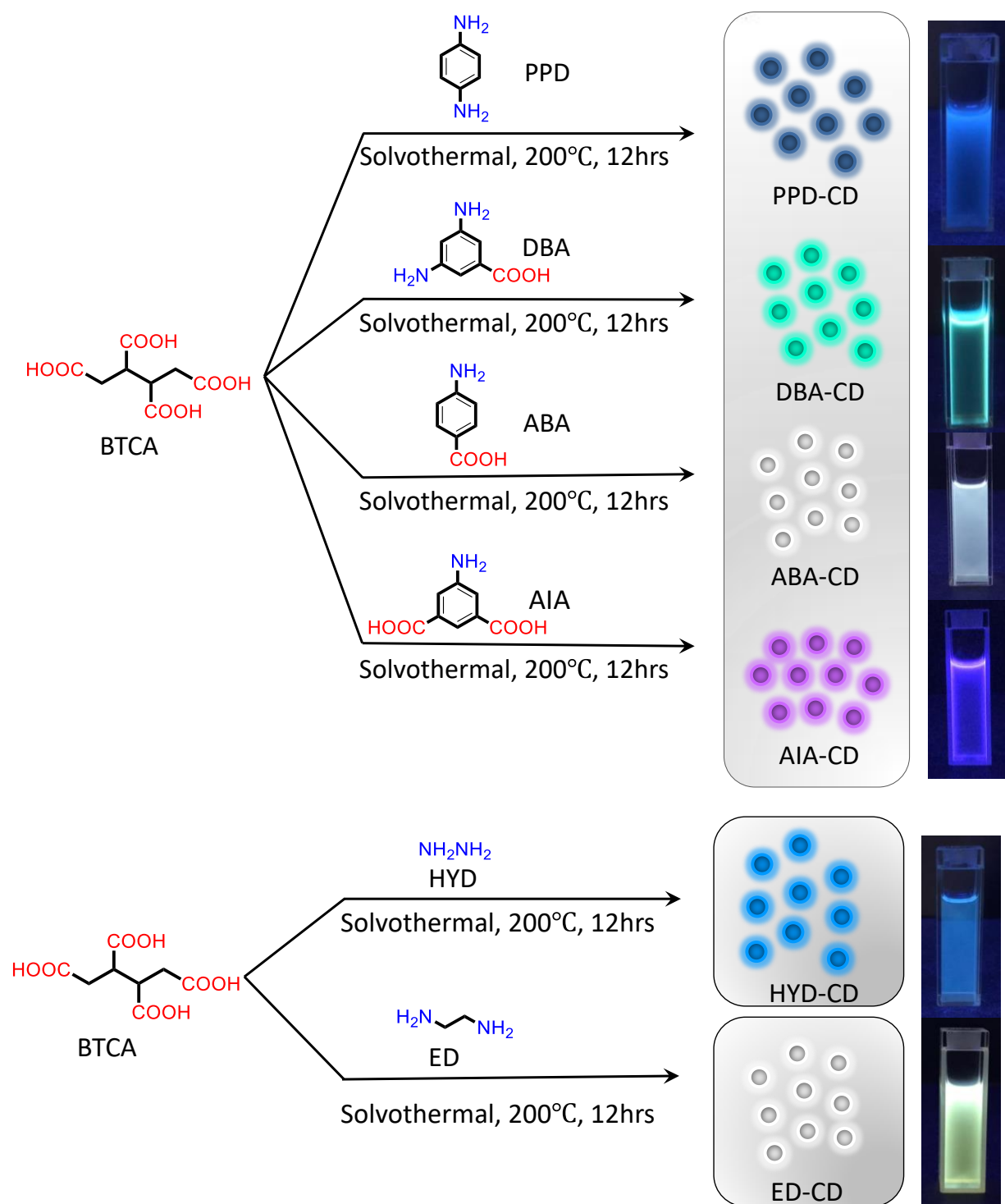


Fig 1. Schematic of the reaction to form **group (1)** PPD-CD, DBA-CD, ABA-CD, and AIA-CD, **group (2)** HYD-CD, and ED-CD.

Chapter 5

Results and Discussions

5.1 Structural Characterization of CD.

Surface structural properties have a crucial impact on the luminescence of CDs. Thus, surface structure and composition of CDs were analyzed by Fourier transform infrared (FTIR) spectra, $^1\text{H-NMR}$, $^{13}\text{C-NMR}$, and Mass Spectroscopy (ESI-MS).

5.1.1 FTIR Analyses

In order to know about the functional groups present on the surface of CDs, FTIR analyses were performed. As shown in Fig 2. All the group 1 carbon dots exhibit -OH, -NH, carboxylic C=O, C=N, sp^2 C=C, C-N, C-O stretching vibration bands in their FT-IR spectra at $3340\text{-}3370\text{ cm}^{-1}$, $3200\text{-}3365\text{ cm}^{-1}$, $1700\text{-}1716\text{ cm}^{-1}$, $1600\text{-}1611\text{ cm}^{-1}$, $1444\text{-}1462\text{ cm}^{-1}$, $1170\text{-}1195\text{ cm}^{-1}$, 1024 cm^{-1} indicating that group 1 carbon dots are simultaneously functionalized by strong electron-donating groups like -OH and -NH₂ and weak electron-withdrawing -COOH groups. The group 2 carbon dots shows stretching vibration peaks corresponding to -OH, -NH, $\text{>C=O/}>\text{C=N}$, C-N, and C-O functional groups at $3265\text{-}3310\text{ cm}^{-1}$, $2870\text{-}3000\text{ cm}^{-1}$, $1640\text{-}1720\text{ cm}^{-1}$, $1220\text{-}1270\text{ cm}^{-1}$, and 1183 cm^{-1} respectively [33].

5.1.2. ^1H and ^{13}C NMR Analyses

In order to get a more clear insight about the functional groups present on the surface of carbon dots along with sp^2 , and sp^3 hybridized carbon domains of the CDs, ^1H and ^{13}C NMR were performed. As shown in Fig 3, in the ^{13}C NMR of CDs, the signals observed in the range of 100 to 180 ppm, and 10-70 ppm are attributed to aromatic domain (sp^2 C), and aliphatic domain (sp^3 C)[34]. The ^{13}C NMR of carbon dots show that the group 1 carbon dots have more content of aromatic region as compared to group 2 carbon dots which have higher aliphatic region. From the ^1H NMR of carbon dots, the peaks in the range of 2-5 ppm confirmed the presence of electron-donating -NH₂ on the surface of CDs. The ^1H NMR spectrums of group 1 carbon dots are more complicated than the group 2 carbon dots, perhaps due to increased polymerization[35]. Further, the ^1H NMR of ED-CD show broad peaks which can be due to its amorphous nature.

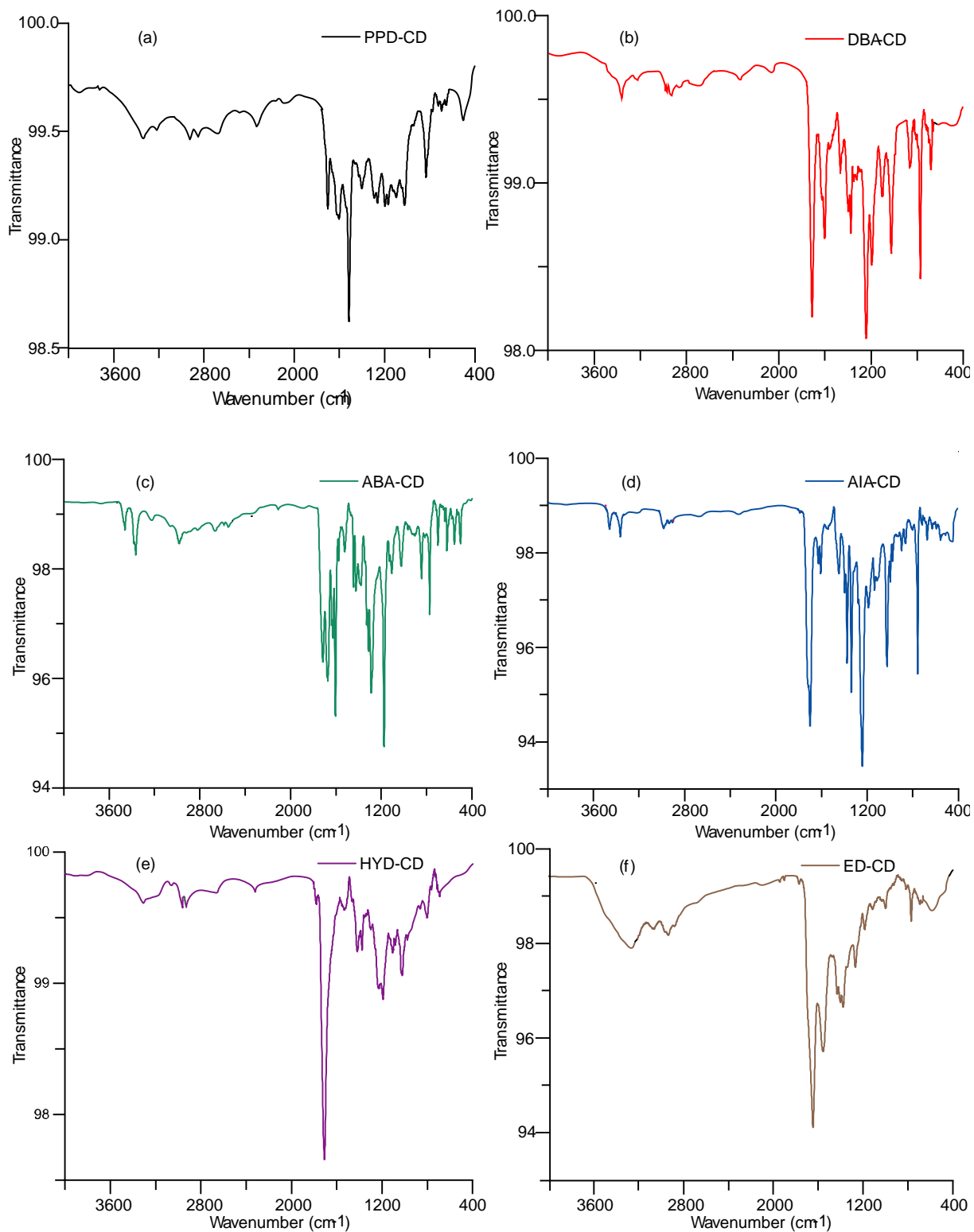


Fig 2. FT-IR Analyses of CDs; (a) PPD-CD, (b) DBA-CD, (c) ABA-CD, (d) AIA-CD, (e) HYD-CD, (f) ED-CD.

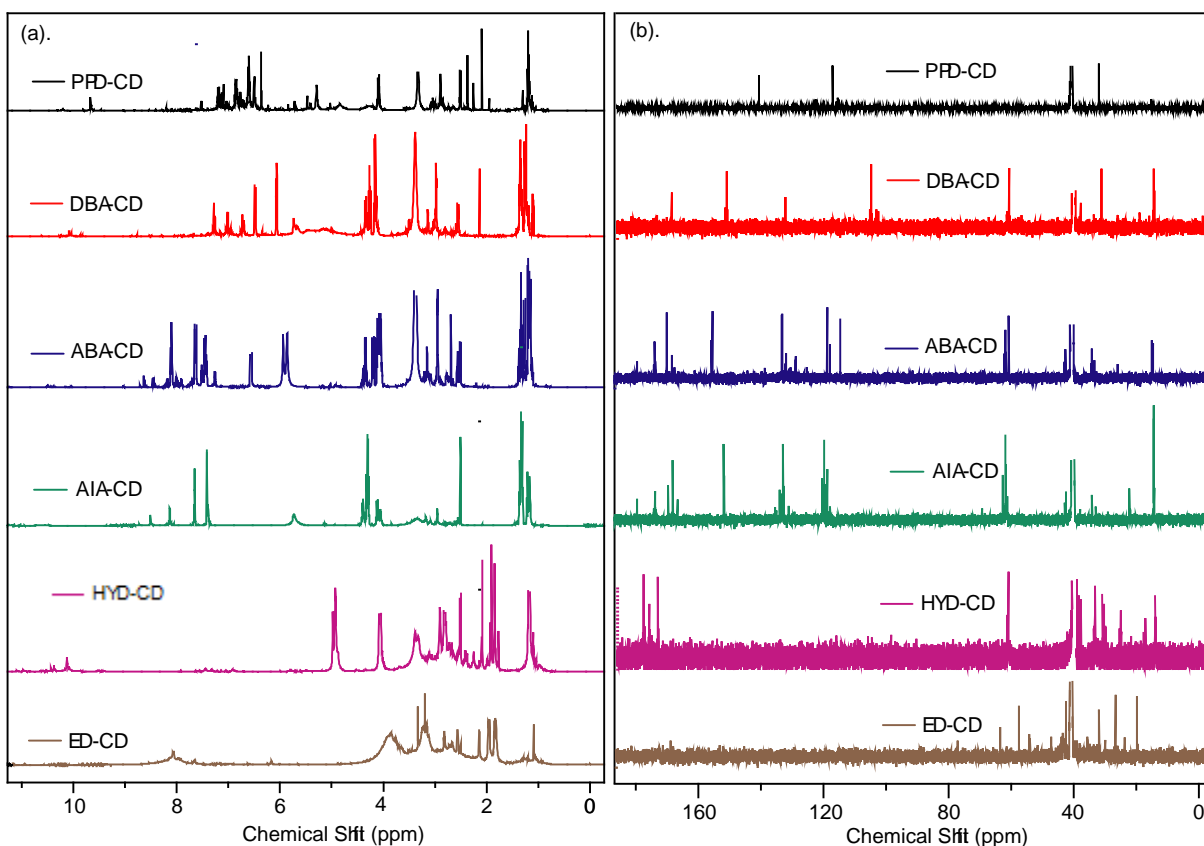


Fig 3. (a) ^1H -NMR, (b) ^{13}C -NMR of PPD-CD (black line), DBA-CD (red line), ABA-CD (blue line), AIA-CD (green line), HYD-CD (purple line), ED-CD (brown line).

5.1.3. Mass Spectroscopic Analyses

In order to further confirm the polymeric structure of the CDs, Mass Spectra are recorded (Fig 4).

Table 1. Mass Spectra Peaks

Samples	Peak	Peak	Peak	Peak	Peak	Peak	Repeating Unit
PPD-CD	(319.1, 347.1)	(369.1, 397.1)	(397.1, 425.1)	(475.2, 447.2)			$-\text{CH}_2-\text{CH}_2-$
DBA-CD	(341.1, 369.1)	(355.1, 383.1)	(407.1, 435.1)	(429.1, 457.1)	(615.2, 643.2)	(637.2, 665.2)	$-\text{CH}_2-\text{CH}_2-$
ABA-CD	(347.1, 383.1)	(369.2, 405.2)	(406.2, 442.2)				H_2O
AIA-CD	(341.1, 369.1)	(392.2, 420.2)	(436.1, 464.1)	(464.1, 492.1)	(523.2, 551.2)		$-\text{CH}_2-\text{CH}_2-$
HYD-CD	(335.1, 353.1)	(361.1, 379.1)	(387.2, 405.2)				$-\text{CH}_2-\text{CH}_2-$
ED-CD	(325.1, 343.1)	(351.2, 369.2)	(547.2, 565.2)	(625.3, 667.3)	(653.3, 671.3)	(689.3, 707.3)	H_2O

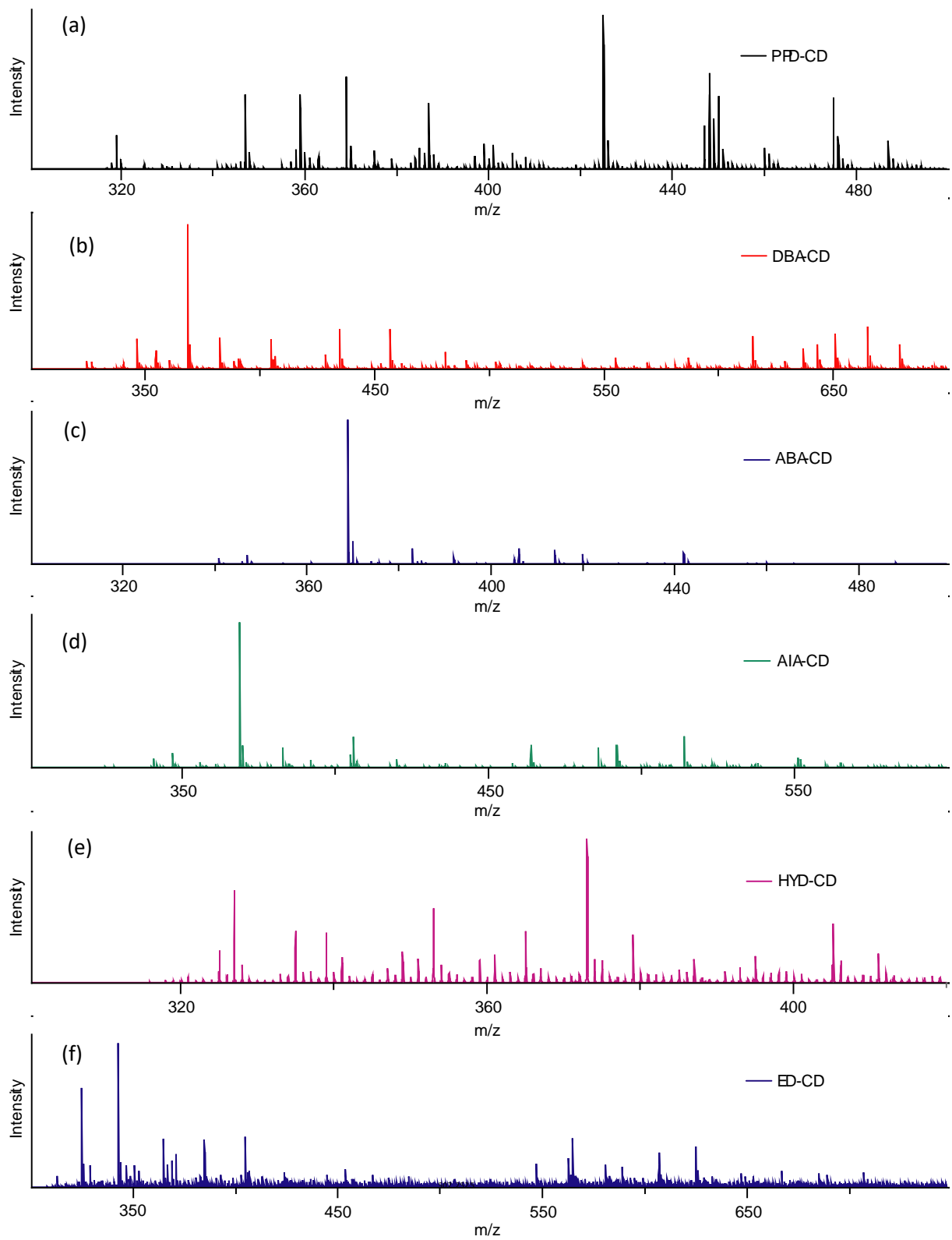


Fig 4. ESI-MS spectra of CDs (a) PPD-CD, (b) DBA-CD, (c) ABA-CD, (d) AIA-CD, (e) HYD-CD, (f) ED-CD.

The ESI-MS Spectra of PPD-CD, DBA-CD, and AIA-CD consist of many 28 fragment ion peaks as shown in Table 1, which illustrates that these CDs contains a large amount of $-\text{CH}_2-\text{CH}_2-$ structure which clearly proves the polymeric structure of the CDs [36]. Moreover, the mass spectra of ABA-CD, ED-CD, and HYD-CD consist of many 36, 18 and 18 fragment ion peaks respectively, which demonstrates that these CDs are probably involved in condensation and dehydration reactions to form conjugated molecules and may have polymeric structures.

5. 2. Morphological Characterization.

In order to get insights of shape and size of the resulting CDs, FESEM analysis was performed over all the dried samples in triplicate (Fig 5). The SEM images of ABA-CD and PPD-CD shows the spherical core shell type structure with average diameter of 20 and 60nm, respectively. Further, the DBA-CD and AIA-CDs shows the spherical structure but later shows the higher degree of aggregation to produce to cluster structures. ED-CD and HYD-CD carbon dots again shows spherical morphology with some cylindrical residues.

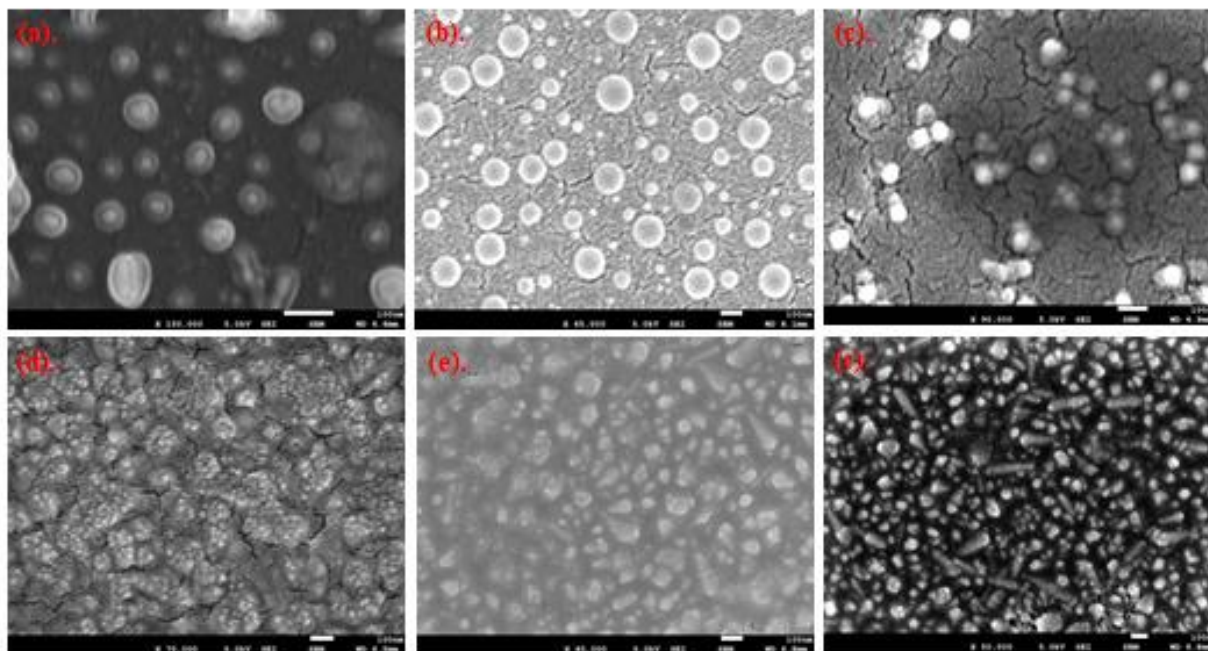


Fig 5. FE-SEM Images of (a). PPD-CD, (b). DBA-CD, (c). ABA-CD, (d). AIA-CD, (e). HYD-CD, (f). ED-CD.

5.3. Optical Characterization

The carbon dots solutions in ethanol exhibit deep-blue (PPD-CD), bluish-green (DBA-CD), white (ABA-CD), purple (AIA-CD), blue (HYD-CD), and yellowish white (ED-CD) colours under 365nm UV light. In order to evaluate the optical properties of the carbon dots, UV-Vis absorption and photoluminescence analyses were conducted.

5.3.1. UV-Vis Absorption Analyses

As shown in Fig. 6, The UV-Vis absorption spectra of DBA-CD, AIA-CD, HYD-CD, ED-CD shows absorption peaks at 200-300 nm which is ascribed to π - π^* transition of C=C/C=N in the sp^2 core, and peaks after 300 nm are attributed to n- π^* transition of C=O/C=N on the surface of CD. The PPD-CD shows π - π^* transition of C=C/C=N in the sp^2 core by showing absorption peak in the range of 200-400 nm, and n- π^* transition of C=O/C=N on the surface of CD due to absorption peaks after 400 nm. The ABA-CD have absorption peaks in the range 200-250 nm, and 270-340 nm because of π - π^* transition of C=C/C=N in the sp^2 core, and n- π^* transition of C=O/C=N on the surface of CD respectively.

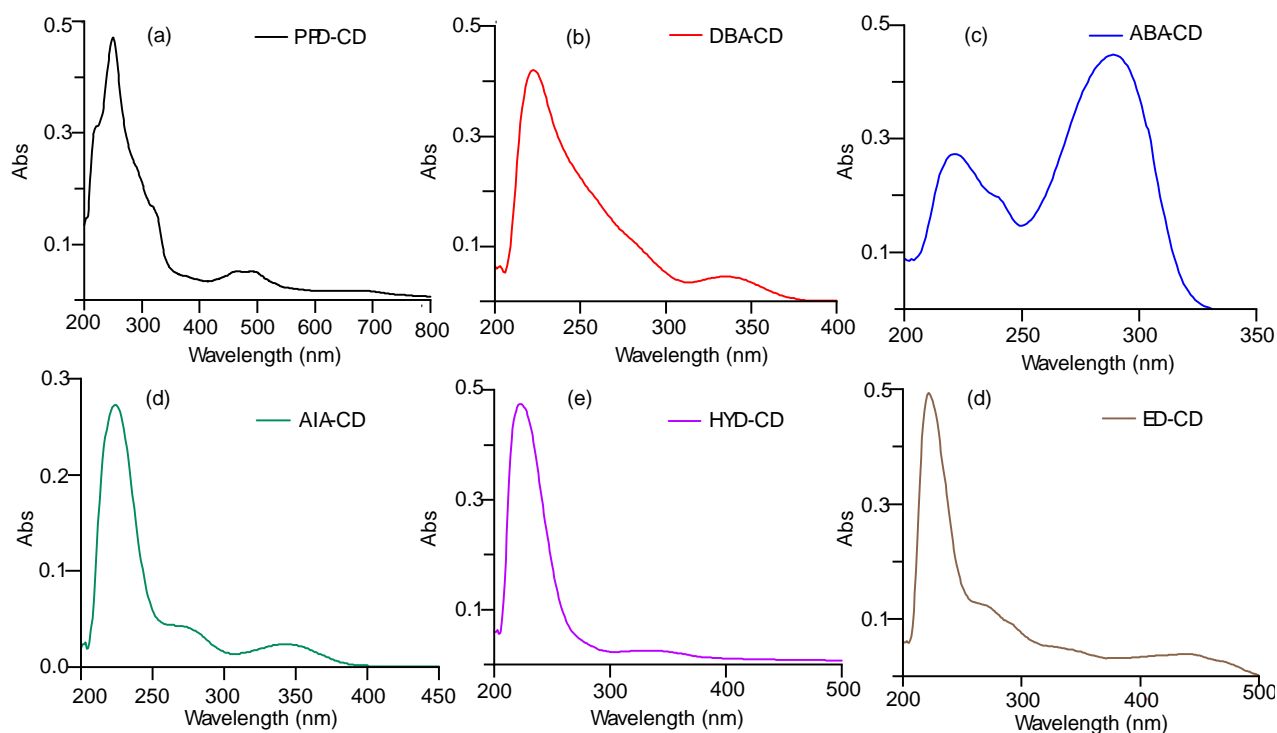


Fig 6. UV-Vis Spectroscopy Curve of (a) PPD-CD, (b)DBA-CD, (c) ABA-CD, (d) AIA-CD, (e) HYD-CD, (f) ED-CD.

5.3.2. Photoluminescence Study

In order to study the photoluminescent behaviour of the CDs, the PL study was conducted. From the PL spectra of CDs shown in Fig7, PPD-CD, DBA-CD, AIA-CD, and HYD-CD displayed maximum emissions at 440nm, 480nm, 420nm, and 455 nm with excitation wavelengths of 360nm, 340nm, 340nm, and 380nm, respectively. The ABA-CD's PL spectrum displayed an emission (exc. 340 nm) covering almost the entire visible region and thus giving white colour fluorescence [37]. The PL spectrum of ED-CD is comprised of two emission peaks- one in blue region and other in green colour region, which, shows that the white colour fluorescence consists of blue, and green colour [38]. The ABA-CD, HYD-CD, and ED-CD exhibit excitation-dependent behaviour which is considered to be due to diverse surface defects caused by nitrogen and oxygen functional groups [39]. The DBA-CD and AIA-CD show excitation independent behaviour indicating fewer surface-state defects [39].

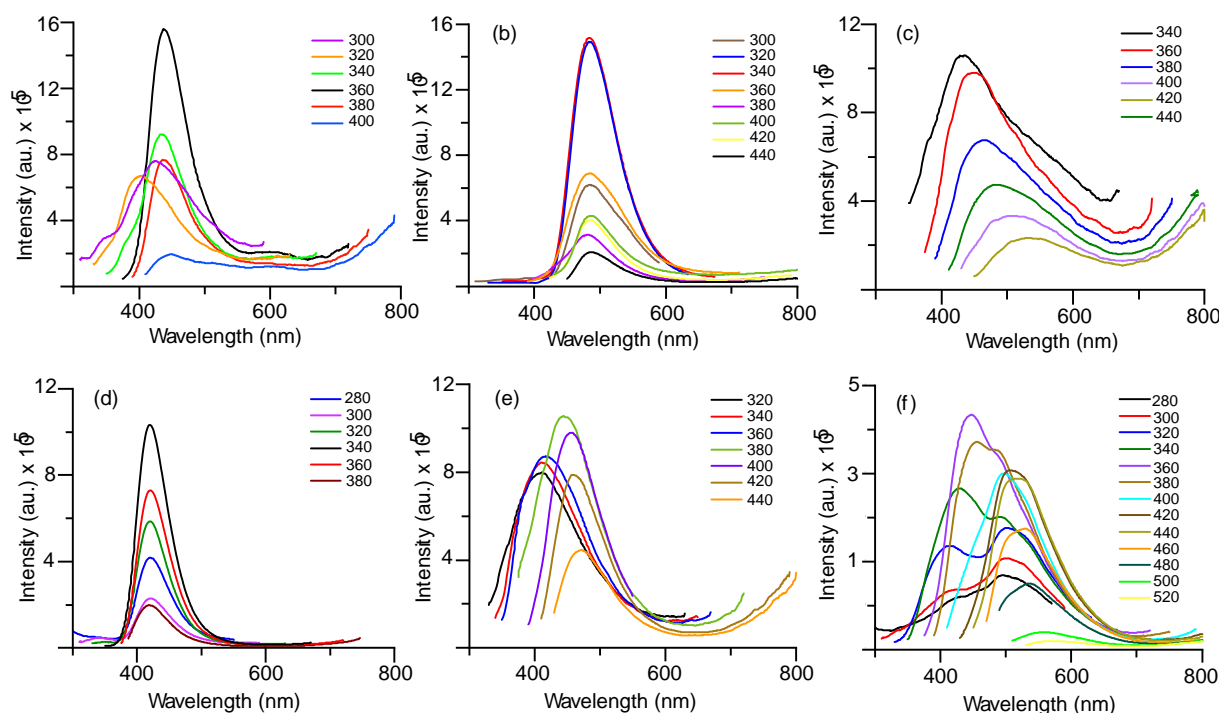


Fig 7. Photoluminescence Spectra of CDs (a). PPD-CD, (b). DBA-CD, (c). ABA-CD, (d). AIA-CD, (e). HYD-CD, (f). ED-CD.

5.3.3. Quantum Yield Measurement

The fluorescence quantum yield at a particular wavelength is defined as the ratio of the number of photons which comes to ground state through fluorescence route to the total number of

photons excited at that particular wavelength. The relative Quantum Yield of carbon dots are calculated by taking a sample with known quantum yield as reference by using the equation [40]:

$$\Phi_s = \Phi_r \times (I_s / I_r) \times (A_s / A_r) \times (\eta_s / \eta_r)^2$$

Where, Subscript “r” and “s”: Reference solution with known Quantum Yield (quinine sulfate in 0.1 M H₂SO₄, $\Phi_r=0.54$) and the samples respectively.

Φ : Fluorescence Quantum Yield

I: Integrated Emission Intensity

A: Optical Absorbance

η : Refractive Index of the dispersive solvent (η_r is 1.33 for DI Water, η_s is 1.36 for Ethanol)

In order to mitigate the interference caused by reabsorption effects, the absorbance at excitation 365nm were maintained less than 0.05[41]. Using the above calculations, the relative fluorescence quantum yield (QY) of PPD-CD, DBA-CD, ABA-CD, AIA-CD, HYD-CD, and ED-CD are calculated to be 1.09%, 29.19%, 8.02%, 37.41%, 14.97%, and 6.43% respectively.

5.3.4. Time Resolved Photoluminescence study

In order to study the nature of fluorophores contributing towards the fluorescence of these carbon dots, along with the nature of energy states present in the CDs, TRPL study is conducted at 334 nm excitation wavelength. The CDs shows average lifetime of 3.91 ns (PPD-CD), 5.31 ns (DBA-CD), 0.86 ns (ABA-CD), 4.80 ns (AIA-CD), 2.21ns (HYD-CD), 3.74ns (ED-CD, λ_{em} : 420 nm), 3.48ns (ED-CD, λ_{em} : 490 nm). The curves were fitted triexponentially for CDs indicating three PL centres except AIA-CD and ED-CD (at λ_{em} 490 nm) were biexponentially fitted indicating two PL centres. Table2. provides information about the lifetimes, and overall contributions of each component in the average lifetime for all CDs. The decay curve of each CD samples consists of a fast component (τ_1 and τ_2 for triexponentially fitted curve, and τ_1 for biexponentially fitted curve) and slow components (τ_3 for triexponentially fitted curve, and τ_2 for biexponentially fitted curve). The fast components are considered to be associated with the radiative recombination of eigenstates, where electrons excitation occurs through $\pi - \pi^*$ transition [42], and fast components which are related to recombination process of the surface states, where electrons excitation occurs through n- π^* transitions [43]. All carbon dots with an exception of DBA-CD have large percentage of fast components. Thus the PL mechanism of DBA-CD is dominated by the surface defect states while the PL mechanism of other carbon dots (PPD-CD,

ABA-CD, AIA-CD, HYD-CD, ED-CD) are dominated by the radiative recombination of the eigenstates.

Table 2. Summary of PL decay curves for CDs

Samples	λ (nm)	τ_1 (ns)	Rel ₁ (%)	τ_2 (ns)	Rel ₂ (%)	τ_3 (ns)	Rel ₃ (%)	τ_{avg} (ns)
PPD-CD	440	0.34	34	1.96	37	10.59	29	3.91
DBA-CD	480	0.84	15	2.49	33	13.73	52	5.31
ABA-CD	430	0.19	29	1.58	66	5.56	5	0.86
AIA-CD	420	4.24	52	5.41	48	-	-	4.80
HYD-CD	450	0.60	44	2.24	43	7.87	12	2.21
ED-CD	420	0.57	37	3.03	34	8.75	28	3.74
ED-CD	490	1.70	59	6.11	40	-	-	3.48

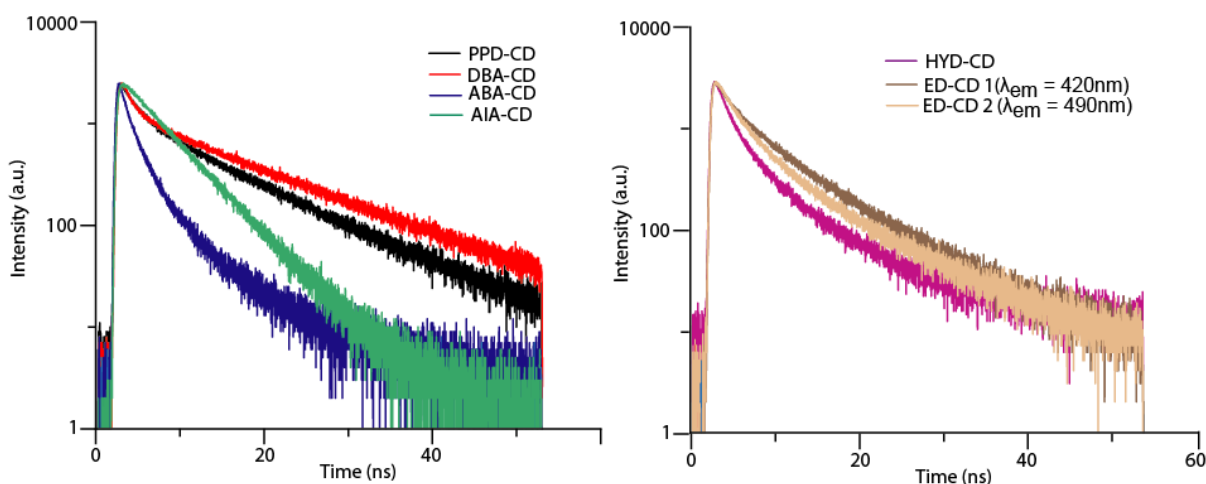


Fig 8. TRPL of PPD-CD (black line), DBA-CD (red line), ABA-CD (blue line), AIA-CD (green line), HYD-CD (purple line), ED-CD 1 (brown line), ED-CD 2 (beige line).

5.3.5. Band Gap Measurements

The AIA-CD, PPD-CD, and DBA-CD showed purple, deep-blue and cyan colour respectively fluorescence under 365 nm UV light. The PL spectra of these carbon dots also exhibited the red shift in their fluorescence. In order to further investigate the mechanism behind the red shift of these carbon dots, the band gap energies of these CDs were calculated from UV-absorption data using Tauc's plot with the formula[44]:

$$(\alpha h\nu)^{\frac{1}{\gamma}} = B(h - E_g)^{\gamma}$$

Where α : Absorption Coefficient ($\alpha = 2.303Acm^{-1}$),

h : Plank Constant

ν : Frequency of the incident photon

γ : depends on the nature of the electronic transition which is equal to $\frac{1}{2}$ or 2 for direct and indirect transition band gaps.

E_g : Energy Band Gap, E_g was calculated using $\gamma = \frac{1}{2}$ for direct electronic transition

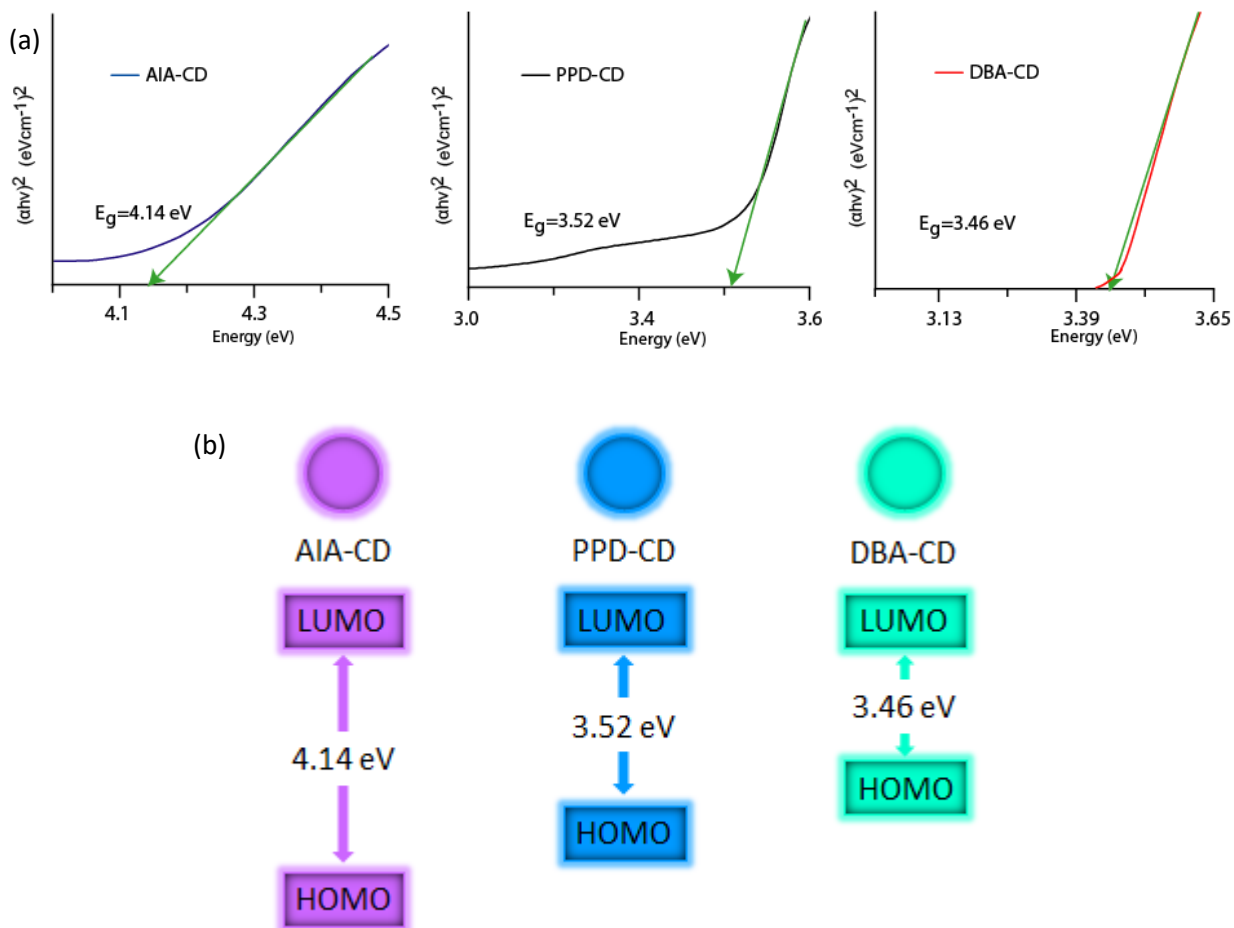


Fig 9. (a) Band Gap Calculations for PPD-CD (black line), DBA-CD (red line), AIA-CD (blue line), (b) illustrative scheme to represent the reduction in bandgap resulting in colour modulation.

Using the above equations and parameters, the band gap energy of AIA-CD, PPD-CD, and DBA-CD were calculated to 4.14 eV, 3.52 eV, 3.46 eV respectively (Fig 9). This trend of reduction in E_g agreed well with the red shift of PL emission wavelengths of these carbon dots. Hence, the red shift in the fluorescence from AIA-CD, PPD-CD, DBA-CD can be attributed to the reduction in the band gap energy.

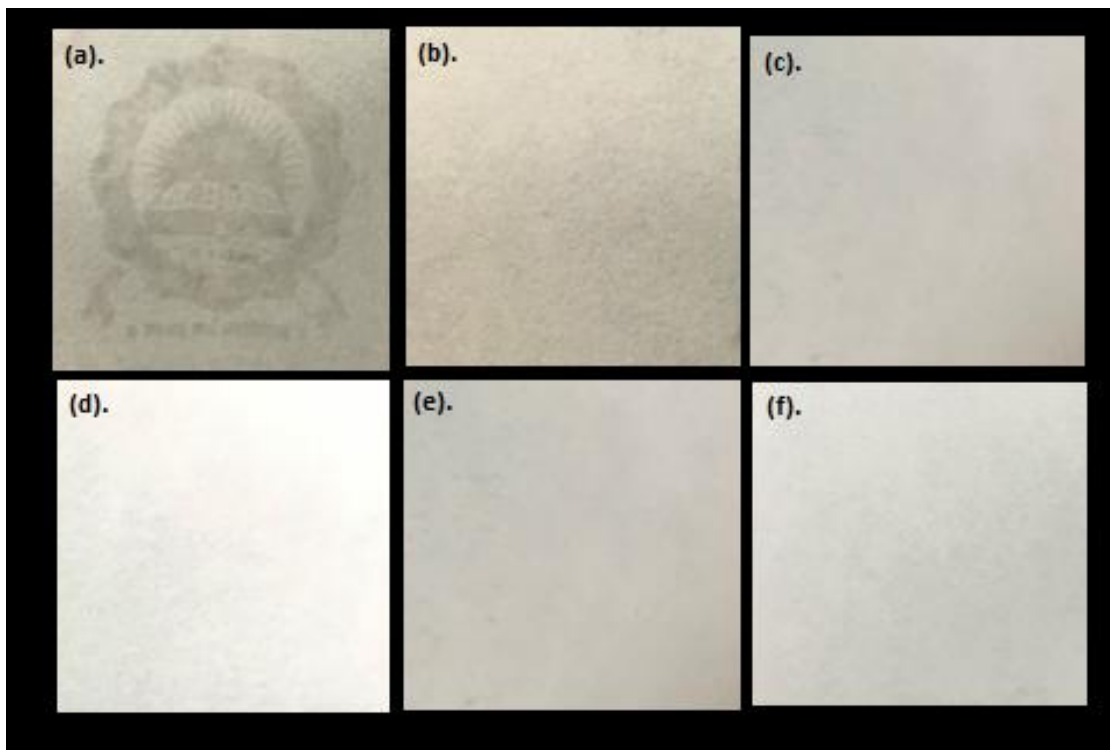
Chapter 6

Applications

6.1. Anti-Counterfeiting Application

These CDs can be utilized in the sector of Anti-Counterfeiting. The experiment was performed using rubber stamp as printing pattern, the carbon dots solution in ethanol was poured onto a stamp pad. Using the stamp, the carbon dots solutions were franked on filter papers. As shown in the Fig 10, stamped pattern is nearly invisible under daylight but shows their respective colour (PPD-CD (deep blue), DBA-CD (cyan), ABA-CD (white), AIA-CD (purple), HYD-CD(blue), ED-CD (yellowish white)) in UV light with a background of blue fluorescence of the filter paper. The stamped pattern maintained its fluorescence even after a week of sunlight exposure which indicated the durability of the stamping material. This technique has the advantage of low cost along with high level of security. These experiments show that these CDs can be used in the field of information protection and anti-counterfeiting owing to their invisibility under daylight, low cost, good stability, easy Processability.

(I)



(II)

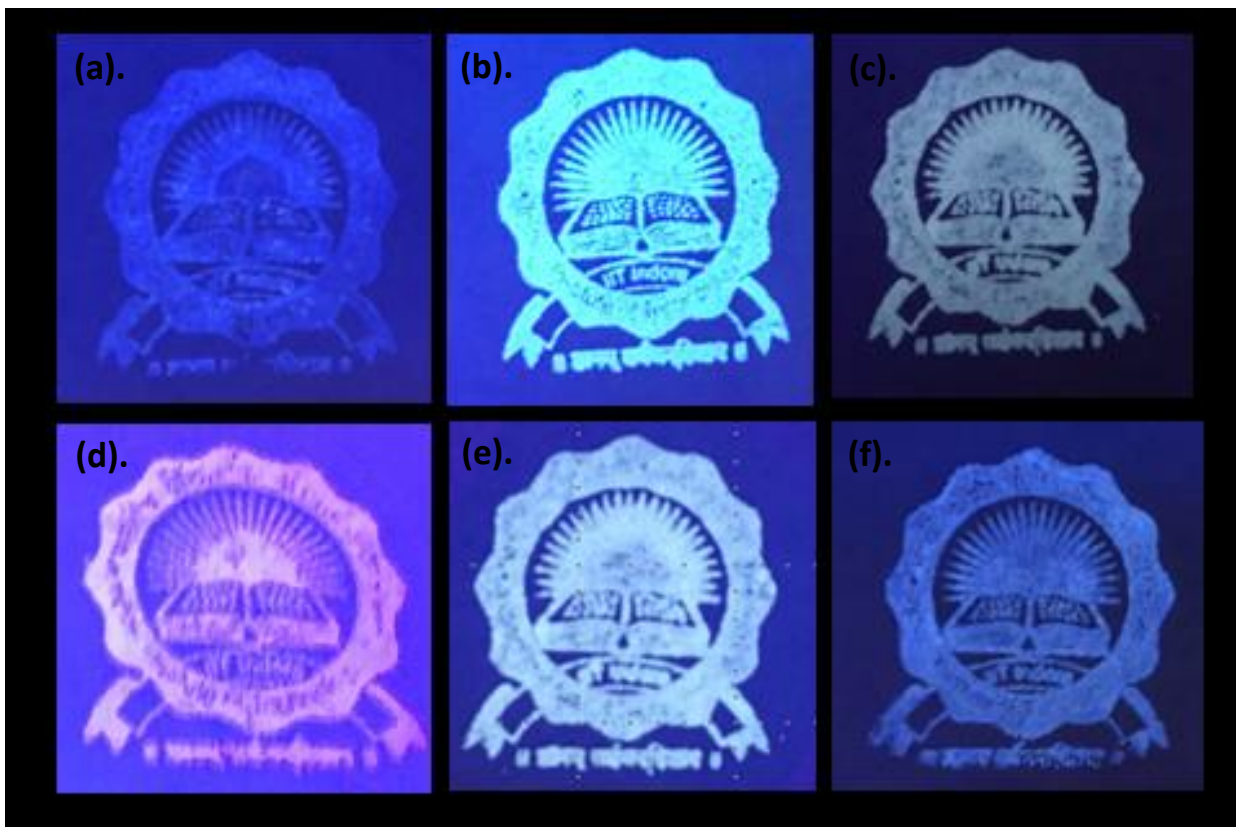
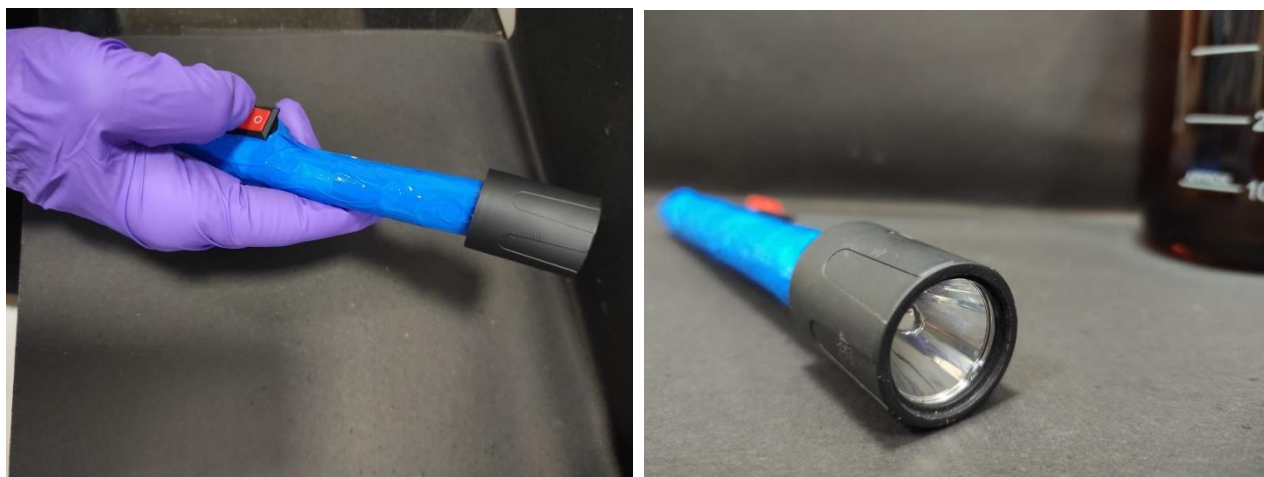


Fig 10. (I) Stamp under Visible light (a). PPD-CD, (b). DBA-CD, (c). ABA-CD, (d). AIA-CD, (e). HYD-CD, (f). ED-CD, (II) Stamp under UV Light (a). PPD-CD, (b). DBA-CD, (c). ABA-CD, (d). AIA-CD, (e). HYD-CD, (f). ED-CD.

6.2. Optoelectronic Application

We have successfully utilized the carbon dots to make a UV Converting Torch which converts UV Light into Visible light showing white, purple, blue, and cyan colour. In order to fabricate the device, carbon dots were mixed with epoxy resin in a volume ratio of 4:1, sonicated for a few minutes to remove the entrapped voids in the solution. All mixtures were heated at 70 °C for 20 minutes followed by cooling at room temperature to obtain epoxy-CD conjugate materials. Further, each solidified products was fixed onto the top of a 365 nm UV LED Chip, which was supplied 4.5 V from a battery. The resultant device converts UV light into the visible light as shown in Fig 11, and gives white, blue, purple, and cyan colour fluorescence, as shown in the figure 12. This application makes the synthesized carbon dots as promising candidates for the optoelectronic devices.

(I)



(II)

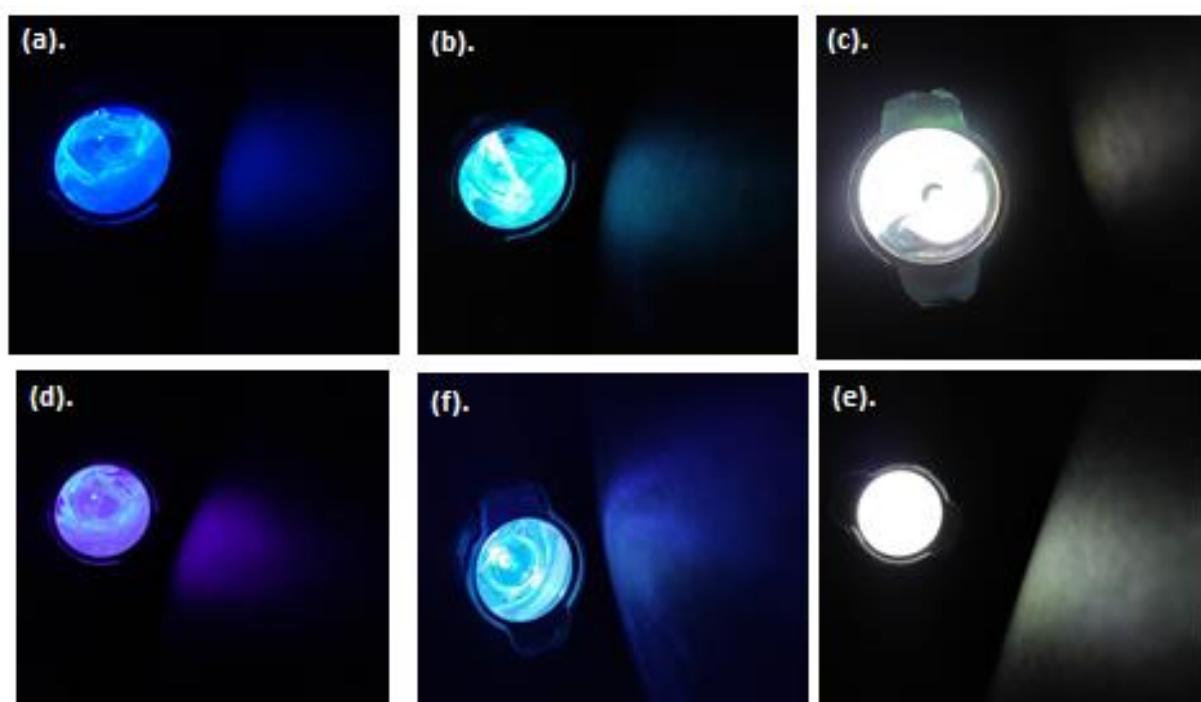


Fig 12.(I) UV Converting (a) Blue Light (PPD-CD), (b) Cyan Light (DBA-CD), (c) White Light (ABA-CD), (d) Purple Light (AIA-CD) (e) Blue Light (HYD-CD) (f). White Light (ED-CD).

Chapter 7

Conclusion and Scope for Future Work

7.1 Conclusion

In summary, the tunable fluorescent CDs are synthesized by Solvothermal reaction of 1, 2, 3, 4-butanetetracarboxylic acid (BTC) with various reagents that fall into two groups: Group 1. Aromatic compounds with different NH_2 : COOH ratio, Group 2. Non Aromatic compounds with different NH_2 : CH_2 ratio. The obtained carbon dots show purple (AIA-CD), blue (PPD-CD, HYD-CD), cyan (DBA-CD), and white colour fluorescence (ED-CD, HYD-CD). ^1H NMR and ESI-MS spectra of these carbon dots show that these carbon dots are formed by polymerization, along with dehydration and condensation reactions in ED-CD, HYD-CD, ABA-CD. The red shift in PL emission wavelength of AIA-CD, PPD-CD, and DBA-CD are coherent with the reduction in the band gaps energy. These CDs are used in the fabrication of torch with varying colours (white, purple, blue, and cyan). Along with optoelectronic devices, these carbon dots are utilized in anti-counterfeiting, and document security application. Owing to low cost, easy synthesis, and stability of CDs, these carbon dots can be used to construct new optoelectronic devices, as well as used in anti-counterfeiting and information storage application.

7.2. Scope for Future Work

In future, further experiments over Carbon Dots can be performed such as Cyclic Voltammetry to get more insight about the undergoing mechanism that's tuning the fluorescence of carbon dots. Along with that, the photoluminescence spectra of white colour emitting carbon dots demonstrates the presence of various colour contributing to white colour photoluminescence. Hence, the silica chromatography can be used to segregate the fluorophores contributing towards the white light. Due to the invisibility of carbon dots under day light, the synthesized carbon dots can be used in defence industries for confidential information storage. Further the obtained carbon dots have high Quantum Yield (37.41% for AIA-CD, 29.19% for DBA-CD) which makes them a promising candidates for bio-imaging, live cell imaging, diagnosis of various diseases.

References

- 1 H. Xiang, R. Wang, J. Chen, F. Li, and H. Zeng, *Light Sci Appl.*, 2021, **10**, 206, 1-16.
- 2 P. Waide, S. Tanishima, and International energy agency Lights labour's lost: Policies for energy efficient lighting, OECD/IEA, Paris, 2006.
- 3 J. Chen, H. Xiang, J. Wang, R. Wang, Y. Li, Q. Shan, X. Xu, Y. Dong, C. Wei, and H. Zeng, *ACS Nano*, 2021, **15**, 17150.
- 4 T. Pulli, T. Dönsberg, T. Poikonen, F. Manoocheri, P. Kärhä and E. Ikonen, *Light Sci Appl.*, 4, 2015, 4.
- 5 W. P. Lustig, Z. Shen, S. J. Teat, N. Javed, E. Velasco, D. M. O'Carroll and J. Li, *Chem. Sci.*, 2020, **11**, 1814.
- 6 M. A. Haar, M. Tachikirt, A. C. Berends, M. R. Krames, A. Meijerink, and F. T. Rabouw, *ACS Photonics*, 2021, **8**, 6, 1784.
- 7 A. Tanaka, R. Sugiura, D. Kawaguchi et. al., *Sci Rep*, 2022, **12**, 7363.
- 8 S. P. Mirasol, E. M. Ferrero and E. Palomares, *Nanoscale*, 2019, **11**, 11315.
- 9 T. V. Medeiros, J. Manioudakis, F. Noun, J. R. Macairan, F. Victoria and R Naccache, *J. Mater. Chem. C*, 2019, **7**, 7175.
- 10 H. Li, X. He, Z. Kang, H. Huang, Y. Liu, J. Liu, S. Lian, C. Tsang, X. Yang, S. Lee, *Angewandte Chemie International Edition*, 2010, **49** (26): 4430.
- 11 F. Wang, L. Wang, J. Xu, K. Huang, and X. Wu, *Analyst*, 2021, **146**, 4418.
- 12 J. Zuo, T. Jiang, X. Zhao, X. Xiao, S. Xiao, and Z. Zhu, *Journal of Nanomaterials*, 2015, **2015**, Article ID 787862.
- 13 X. Y. Shan, L. J. Chai, J. J. Ma, Z. S. Qian, J. R. Chena and H. Feng, *Analyst*, 2014, **139**, 2322–2325.
- 14 B. De, and N. Karak, *RSC Adv.*, 2013, **3**, 8286–8290
- 15 Q. Liu,* X. Niu, K. Xie, Y. Yan, B. Ren, R. Liu, Y. Li, and L. Li, *ACS Appl. Nano Mater.*, 2021, **4**(1), 190.
- 16 Y. Deng, Q. Li, Y. Zhou, and J. Qian, *ACS Appl. Mater. Interfaces*, 2021, **13**, 57084–57091
- 17 V. Mehta, S. Jha, R. Singhal and S. Kailasa, *New J. Chem.*, 2014,**38**, 6152-6160
- 18 J. Chen, J. Wei, P. Zhang, X. Niu, W. Zhao, Z. Zhu, H. Ding, and H. Xiong, *ACS Appl. Mater. Interfaces*, 2017, **9**, 18429–18433.
- 19 S. Zhang, L. Yuan, G. Liang and A. Gu, *J. Mater. Chem. C*, 2022, DOI: 10.1039/D2TC00789D.

- 20 K. Yuan, X. Zhang, R. Qin, X. Ji, Y. Cheng, L. Li, X. Yang, Z. Lu and H. Liu, *J. Mater. Chem. C*, 2018, **6**, 12631.
- 21 W. Li, M. Wu, H. Jiang, L. Yang, C. Liu and X. Gong, *Chem. Commun.*, 2022, **58**, 1910.
- 22 D. Zhou, D. Li, P. Jing, Y. Zhai, D. Shen and S. Qu, *Chem. Mater.*, 2017, **29**, 1779.
- 23 Y. Zhao, C. Ou, J. Yu, Y. Zhang, H. Song, Y. Zhai, Z. Tang and S. Lu, *ACS Appl. Mater. Interfaces*, 2021, **13**, 30098.
- 24 D. Chen, H. Gao, X. Chen, G. Fang, S. Yuan and Y. Yuan, *ACS Photonics*, 2017, **4**, 2352.
- 25 Y. Deng, D. Zhao, X. Chen, F. Wang, H. Song and D. Shen, *Chem. Commun.*, 2013, **49**, 5751.
- 26 J. Liu, R. Li, and B. Yang, *ACS Cent. Sci.*, 2020, **6**, 2179.
- 27 A. Tyagi, K. Tripathi, N. Singh, S. Choudharya, and R Gupta, *RSC Adv.*, 2016, **6**, 72423–72432
- 28 Z. Ye, G. Li, J. Lei, M. Liu, Y. Jin, and B. Li, *ACS Appl. Bio Mater.*, 2020, **3**, 7095.
- 29 Y. An, X. Lin, Y. Zhou, Y. Li, Y. Zheng, C. Wu, K. Xu, X. Chai, C. Liu, *RSC Adv.*, 2021, **11**, 26915-26919
- 30 H. Ding, S. Yu, J. Wei, and H. Xiong, *ACS Nano*, 2016, **10**, 484
- 31 N. Nandi, P. Sarkar, and K. Sahu, *ACS Appl. Nano Mater.*, 2021, **4**, 9616
- 32 T. Yuan, F. Yuan, X. Li, Y. Li, L. Fan, and S. Yang, *Chem. Sci.*, 2019, **10**, 9801.
- 33 V. Strauss, H. Wang, S. Delacroix, M. Ledendecker, and P. Wessig, *Chem. Sci.*, 2020, **11**, 8256.
- 34 L. Zhu, D. Shen, Q. Wang, and K. Luo, *ACS Appl. Mater. Interfaces*, 2021, **13**, 56465.
- 35 B. Wang, H. Song , Z. Tang, B. Yang, S. Lu, *Nano Res.*, 2022, **15(2)**, 942
- 36 K. De, A. Welle, S. Hirth, S. J. Blanksby, C Barner. *Nat. Rev. Chem.*, 2020, **4**, 257.
- 37 Wang et al., *Sci. Adv.*, 2020, **6**, 1.
- 38 W. Li, M. Wu, H. Jiang, L. Yang, C. Liu, and X. Gong, *Chem. Commun.*, 2022, **58**, 1910.
- 39 Z. Yang., M. Xu, Y. Liu, F. He, F. Gao, Y. Su, H. Wei, Y. Zhang, *Nanoscale*, 2014, **6**, 1890.
- 40 L. Guo, Y. Zhang, and W. Li, *Journal of Colloid and Interface Science*, 2017, **493**, 257–264

- 41 S. Jing, Y. Zhao, R. Sun, L. Zhong, X. Peng, *ACS Sustainable Chem. Eng.* 2019, **7**, 7833.
- 42 X. Li, S. Lau, L. Tang, R. Ji, P. Yang, *Nanoscale*, 2014, **6**, 5323
- 43 T. Zhang, J. Zhu, Y. Zhai, H. Wang, X. Bai, B. Dong, H. Wang, H. Song, *Nanoscale*, 2017, **9**, 13042.
- 44 G. Nocito, E. Luigi Sciuto, and D. Franco et.al, *Nanomaterials*, 2022, **12**, 885